

Production of a nuclearly polarized ${}^3\text{He}^+$ beam by multiple electron capture and stripping collisions

M. Tanaka,¹ T. Yamagata,² K. Yonehara,² T. Takeuchi,² Y. Arimoto,³ M. Fujiwara,³ Y. Plis,⁴ L. W. Anderson,⁵ and R. Morgenstern⁶

¹Kobe Tokiwa Junior College, Ohtani-cho 2-6-2, Nagata-ku, Kobe 653-0838, Japan

²Department of Physics, Konan University, Okamoto 8-9-1, Higashinada 658-8501, Kobe, Japan

³Research Center for Nuclear Physics, Osaka University, Mihogaoka 10-1, Ibaraki, Osaka 567-0024, Japan

⁴Joint Institute for Nuclear Research, Dubna, Moscow, Russia

⁵Department of Physics, University of Wisconsin, 1150 University Avenue, Madison, Wisconsin 53706

⁶KVI, The University of Groningen, Zernikelaan 25-9747 AA, Groningen, The Netherlands

(Received 28 April 1999)

A ${}^3\text{He}^+$ beam with nuclear polarization was produced by passing a fast ${}^3\text{He}^+$ -ion beam through a thick polarized Rb vapor target in a strong magnetic field. Observed polarization transfer coefficients as a function of the Rb vapor thickness are qualitatively explained by an electron pumping model based on multiple processes of electron capture and stripping. The experimentally obtained polarization and beam current for the ${}^3\text{He}^+$ beam were, respectively, 0.07 and $2\ \mu\text{A}$ for a Rb polarization of 0.2. [S1050-2947(99)51111-6]

PACS number(s): 34.80.Nz, 13.88.+e

In recent years, nuclear polarized ${}^3\text{He}$ gases and ions have received growing attention in a variety of scientific fields from quark physics to life science [1]. Historically, a number of methods have been attempted for the production of polarized ${}^3\text{He}$ ions and atoms. Polarized ${}^3\text{He}$ atoms have been successfully produced by both metastability exchange optical pumping [2] and spin exchange optical pumping [3,4].

On the other hand, the production of polarized ${}^3\text{He}$ ions has not been as thoroughly developed as is the production of polarized ${}^3\text{He}$ atoms. The first method used to produce polarized ${}^3\text{He}^+$ ions was realized by extracting polarized ${}^3\text{He}^+$ ions from a discharge in a metastability exchange pumped cell [5]. According as the ions are extracted, resonant charge-exchange collisions may enhance the polarization. The ${}^3\text{He}^+$ polarization and beam current realized by this method were 0.11 and $8\ \mu\text{A}$, respectively [6]. The second method for producing the polarized ${}^3\text{He}^{2+}$ ions was based on the Lamb-shift method [7,8]. The polarization and beam current achieved by this method were almost 0.7 and $4\ \mu\text{A}$.

For polarized H^- ions, significant advantages are obtained for both the beam current and beam emittance by using charge changing collisions between fast incident ions and polarized alkali-metal atoms to produce the polarized ions [9,10]. This method, called OPPIS (optically pumped polarized ion source), uses an optically pumped polarized alkali-metal vapor for the charge-exchange medium. Tanaka *et al.* [11] have studied the application of this technique to the production of nuclear polarized ${}^3\text{He}$ ions. An outgrowth of this study was an idea for producing polarized ${}^3\text{He}$ by multiple capture and stripping collisions between optically pumped polarized Rb atoms and a fast ${}^3\text{He}$ beam [12]. We called this method "electron pumping" in analogy with the principle of optical pumping [13,14]. In this paper, we first discuss the physics of electron pumping and then present the experimental results and interpretation in terms of a model based on the electron pumping.

Figure 1(a) illustrates an intuitive explanation of the method. An unpolarized ${}^3\text{He}^+$ ion beam with an energy of a few keV/A is incident on a polarized alkali-metal vapor target from the left. Major processes at this energy are electron capture for ${}^3\text{He}^+$ ions and electron stripping for ${}^3\text{He}$ atoms,

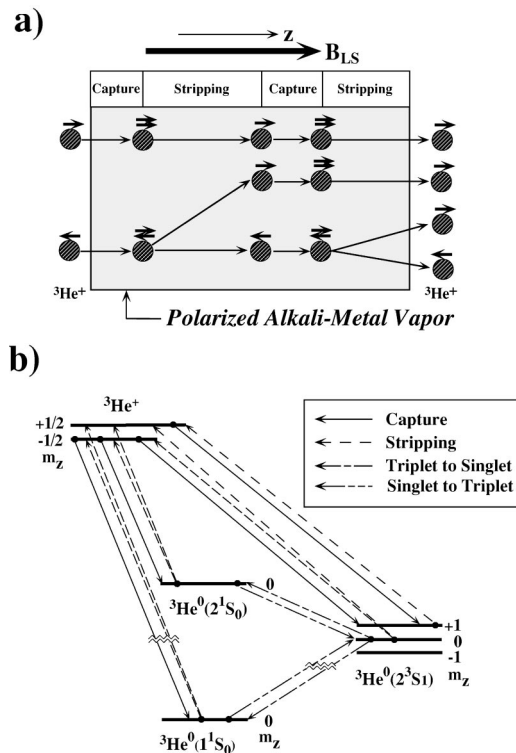


FIG. 1. Principle of electron pumping. (a) An unpolarized ${}^3\text{He}^+$ ion incident on a polarized Rb atom captures a polarized electron followed by the stripping of one of the two electrons in the ${}^3\text{He}$ atom. By repeating this cycle a number of times, the degree of ${}^3\text{He}^+$ polarization increases. Arrow lengths qualitatively give mean-free paths for a ${}^3\text{He}^+$ ion and ${}^3\text{He}$ atom. (b) Schematic explanation of electron pumping in analogy with optical pumping.

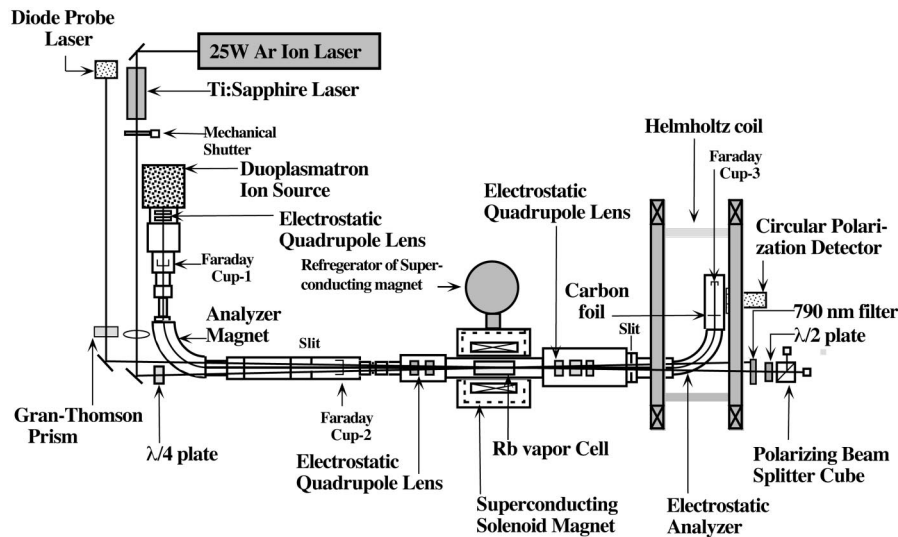


FIG. 2. Experimental setup. A ${}^3\text{He}^+$ -ion beam produced by a duoplasmatron is incident on a Rb vapor cell located along the axis of a 2-T superconducting magnet. The emerging ${}^3\text{He}^+$ is transported to a polarimeter after passing through a 90° electrostatic analyzer. To maintain the polarization, a guiding field is applied to the region of the polarimeter and the electrostatic analyzer. The principle of the polarimeter is based on a beam-foil spectroscopy as described in the text.

while an electron stripping of a ${}^3\text{He}^+$ ion to form a ${}^3\text{He}^{2+}$ ion, an electron capture of a ${}^3\text{He}$ atom to form a ${}^3\text{He}^-$ ion, or a two-electron capture of a ${}^3\text{He}^+$ ion to form a ${}^3\text{He}^-$ ion is negligibly small. As a result, only successive processes of electron capture for ${}^3\text{He}^+$ ions and stripping for ${}^3\text{He}$ atoms are significant. An incident ${}^3\text{He}^+$ ion first captures a polarized electron from an alkali-metal atom forming an excited ${}^3\text{He}$ atom, followed by deexcitation either to the ground or metastable state by radiative decay. A 2-T decoupling field, B_{LS} is applied to the collision region to avoid the depolarization of the captured electron during radiative decay. During further passage of the ${}^3\text{He}$ atom through the polarized alkali-metal vapor, the ${}^3\text{He}$ atom is converted into a ${}^3\text{He}^+$ ion again by an electron stripping process. Since either of the two electrons of the ${}^3\text{He}$ atom can be stripped with approximately the same probability, the ${}^3\text{He}^+$ ion is polarized by this process. If the alkali-metal vapor thickness is large enough to allow repeated capture and stripping cycles, the polarization of the ${}^3\text{He}^+$ ion increases and finally reaches a maximum value determined by the polarization of the alkali-metal vapor.

The multiple-collision processes mentioned above can be discussed in another way. An energy-level diagram for a ${}^3\text{He}^+$ ion and a ${}^3\text{He}$ atom is shown in Fig. 1(b), where the levels of the ${}^3\text{He}$ atom with $S=0$ (singlet levels, S) and with $S=1$ (triplet levels, T) are indicated. An incident ${}^3\text{He}^+$ ion first captures a polarized electron from an alkali-metal atom and forms a ${}^3\text{He}$ atom in an excited state. It then deexcites to the ground or metastable state of the ${}^3\text{He}$ atom by radiative decay. The radiative decay keeps the spin multiplet unchanged. Figure 1(b) shows the energy levels of the ${}^3\text{He}^+$ ion, including the two metastable levels and the ground level of the ${}^3\text{He}$ atom. Other levels are not shown for simplicity. In the capture process, a ${}^3\text{He}^+$ ion with an $m_z = +\frac{1}{2}$ magnetic substate captures a polarized electron to form only a ${}^3\text{He}(T)$ atom with $m_z = +1$, while a ${}^3\text{He}^+$ ion with $m_z = -\frac{1}{2}$ captures a polarized electron and forms either a ${}^3\text{He}(T)$ or a ${}^3\text{He}(S)$ state with $m_z = 0$. When an electron stripping process takes place, a ${}^3\text{He}^+$ ion is formed again. An electron stripping process for the ${}^3\text{He}(T)$ atom with $m_z = +1$ forms only a ${}^3\text{He}^+$ ion with $m_z = +\frac{1}{2}$, while an electron stripping for the ${}^3\text{He}(T)$ or ${}^3\text{He}(S)$ atom with $m_z = 0$ forms

a ${}^3\text{He}^+$ ion with $m_z = +\frac{1}{2}$ or $-\frac{1}{2}$ with equal probability. Most of the ${}^3\text{He}$ singlet atoms are in the ground level. The electron stripping process from this level is negligibly small at our incident energy. After many repetitions of the capture and stripping processes, the ${}^3\text{He}^+$ ions with $m_z = +\frac{1}{2}$ predominate; that is, the electron of the ${}^3\text{He}^+$ ion is polarized. The above scenario is almost identical to the principle of optical pumping if one replaces a polarized electron with a circularly polarized photon. This is the reason why we name our method electron pumping. It should be further mentioned that the electron pumping requires large-collision cross sections for both capture and stripping processes. In fact, this condition is satisfied for a fast ${}^3\text{He}$ ion incident on a Rb target, as will be discussed later.

Figure 2 shows the apparatus constructed at RCNP, Osaka University. A 19-keV ${}^3\text{He}^+$ ion beam is extracted from a duoplasmatron ion source and is incident on a 32-cm-long Rb vapor cell. The Rb vapor cell is located in a 2-T axial magnetic field supplied by a superconducting solenoidal coil. The Rb cell temperature is varied from 100 to 120 $^\circ\text{C}$ with a precision better than 0.1 $^\circ\text{C}$ to change the Rb vapor thickness from 1×10^{14} to 6×10^{14} atoms/cm 2 . The Rb vapor is polarized using the D_1 transition of the Rb atom (795 nm) with a 4-W Ti:sapphire laser pumped by a 25-W Ar-ion laser. The linewidth of the pumping laser is ~ 20 GHz, which is sufficient to fully cover the linewidth caused by the Doppler broadening and inhomogeneity of the solenoidal magnetic field. We use the Faraday effect to monitor the thickness and polarization of the Rb vapor P_{Rb} by using linearly polarized 790-nm light provided from a diode probe laser. It is found that P_{Rb} decreases from 0.6 to 0.2 with an increase of the Rb thickness from 2×10^{14} to 10×10^{14} atoms/cm 2 . To understand this behavior in more detail, a direct observation of the Rb depolarization was done using a chopped pumping laser [15].

The ${}^3\text{He}^+$ ions emerging from the Rb vapor cell become partially nuclear polarized by the hyperfine interaction when they reach a region where the external magnetic field is small. The ${}^3\text{He}$ nuclear polarization P_N is half of the electron polarization P_e of the ${}^3\text{He}^+$ ion in the strong magnetic field [16]. The nuclear polarized ${}^3\text{He}^+$ ions are then separated from the fast ${}^3\text{He}$ atoms by a 90° electrostatic analyzer

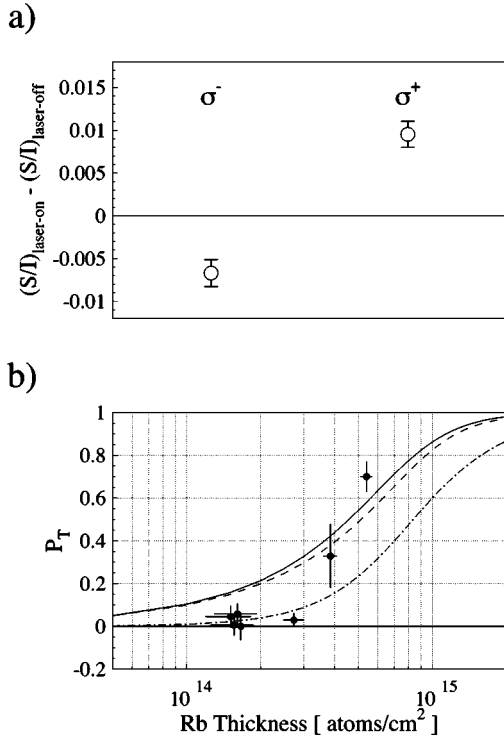


FIG. 3. (a) Observed Stokes parameters corrected for the baseline shift due to the system asymmetry. σ^+ (σ^-) indicates the right (left) circular polarization for the pumping laser, respectively. (b) Experimental and theoretical values of the polarization transfer coefficient P_T plotted as a function of the Rb vapor thickness. P_T is defined as a $P_{^3\text{He}}/P_{\text{Rb}}$, where $P_{^3\text{He}}$ is an electron polarization of the $^3\text{He}^+$ ion after emerging from the polarized Rb vapor.

and enter a polarimeter for the measurement of the ^3He nuclear polarization by means of a beam-foil spectroscopy [17]. To preserve the direction of the ^3He polarization, a weak magnetic field ($B \sim 10$ G) from a Helmholtz coil is applied to the region of the electrostatic analyzer and the polarimeter. We observe a circular polarization of the 389-nm photons corresponding to the transitions between the $3^3P_J (J=0,1,2)$ and 2^3S_1 states in the ^3He I atom set in flight by the polarimeter. The 389-nm photons predominate among the observed ones and were successfully used for our previous measurements [11,18].

Figure 3(a) shows the observed normalized Stokes parameter, S/I taken for the 389-nm photons at the Rb vapor thickness of 5.3×10^{14} atoms/cm². Here, S/I is defined as $S/I = [I(\sigma^+) - I(\sigma^-)] / [I(\sigma^+) + I(\sigma^-)]$ with $I(\sigma^+)$ and $I(\sigma^-)$ = intensity for the right- and left-hand circularly polarized photon in the optical convention, respectively. S/I is also expressed in terms of the ^3He nuclear polarization, P_N by

$$S/I = AP_N, \quad (1)$$

where A is a time-averaged analyzing power for the 389-nm photons and is evaluated to be $A = 0.207$ [11]. σ^+ (σ^-) in Fig. 3(a) indicates right (left) circular polarization for the pumping laser, respectively. To correct the instrumental asymmetry, S/I taken without the pumping laser is subtracted from S/I with the pumping laser. The experimental result clearly demonstrates that the polarimeter satisfactorily

TABLE I. Cross sections for capture, stripping, atomic transitions between a triplet and singlet state, and spin exchange used for the calculations of P_T as a function of the Rb thickness. The cross sections are in units of 10^{-14} cm².

Curve	σ_{+t}	σ_{+s}	σ_{t+}	σ_{s+}	σ_{ts}	σ_{st}	σ_{ex}
Solid	0.230	0.092	0.108	0.0012	0.038	0.0022	0.1
Dashed	0.230	0.092	0.059	0.0012	0.038	0.0022	0.1
Dot-dashed	0.230	0.092	0.108	0.0012	0.038	0.0022	0.0

works because S/I changes its sign when circular polarization of the pumping laser is changed. P_N is extracted from the observed S/I and A .

Figure 3(b) shows the observed polarization transfer coefficient P_T taken at different Rb vapor thicknesses. Here, P_T is defined by P_e/P_{Rb} , where P_e is evaluated by doubling P_N determined from Eq. (1). The P_T error bars indicated are mainly due to uncertainty in the measurement of the Faraday rotation angle and counting statistics. The observed P_T 's in Fig. 3(b) clearly demonstrate an increase with the increase of the Rb vapor thickness.

The experimental results are compared with the theoretical calculations for the electron pumping. The rate equations prescribed in Ref. [12] are improved and solved with a few sets of the reasonable collision cross sections. Since adequate data are not available for the Rb + ^3He system, we use data deduced from the charge-exchange collisions between cesium vapor and ^4He ions at $E(^4\text{He}) = 25$ keV [19], expecting that the cross sections for the Rb + ^3He system are similar to the ones above [21]. Since the presence of the spin-exchange interactions between a Rb atom and a ^3He atom or a $^3\text{He}^+$ ion is expected to enhance the electron pumping, we employ the spin-exchange cross section theoretically predicted for a fast hydrogen incident on a rubidium atom [20]. More reliable estimates of the spin-exchange cross sections are needed for the $^3\text{He}^+ + \text{Rb}$ system. For this purpose, theoretical calculations of it are done and will be presented elsewhere [22].

The solid curve is the result of the full calculation, and the dot-dashed and dashed curves are, respectively, the calculated result with the spin-exchange cross section set equal to zero and the result with the stripping cross section σ_{t+} reduced to a half of the first case. The need for the third calculations (dashed curve) is due to the fact that the measurement of the stripping cross section of a ^4He atom in either a triplet or singlet state has an uncertainty larger than that of the capture cross section because of the indirect measurement [19]. The numerical values of the cross sections for the above three cases are shown in Table I. Here, σ_{+t}, σ_{+s} are the capture cross sections for a $^3\text{He}^+$ ion forming ^3He in triplet and singlet metastable levels, respectively. σ_{t+} and σ_{s+} are, respectively, the stripping cross section for a ^3He atom in the triplet and the singlet levels forming a $^3\text{He}^+$ ion. σ_{ts}, σ_{st} are the cross sections for atomic transitions from a triplet to singlet state and vice versa. σ_{ex} is a spin exchange cross section between a Rb atom and a ^3He atom or a $^3\text{He}^+$ ion. The calculated results in Fig. 3(b) demonstrate that the increase of P_T , as the Rb vapor thickness increases, is not extremely sensitive to the absolute values of the stripping cross sections, and that the effect of the electron pumping is,

in fact, enhanced by the presence of the spin-exchange collisions. Though more precise experimental data are needed for a further detailed comparison with the theory of electron pumping, one can conclude that the basic principle is qualitatively verified in the present measurement. It is of particular importance to note that the stripping cross sections for a ^3He atom are exceptionally large as compared with the hydrogen case [23], which leads to the success of electron pumping for ^3He .

The maximum values of $^3\text{He}^+$ nuclear polarization and beam intensity obtained here are, respectively, 0.07 and 2

μA [24]. These values could be greatly improved by further instrumental development; for example, use of an ECR (electron cyclotron resonance) ion source instead of the duoplasmatron, a SONA field [16], and a longer geometry of the Rb cell region.

This work has been performed with the support of the Research Center for Nuclear Physics (RCNP) Cyclotron Facility at Osaka University and a Grant-in-Aid from the Ministry of Education of Japan. The authors wish to express their sincere appreciation to Professor H. Ejiri for his encouragement throughout this work.

-
- [1] Proceedings of the International Workshop on Polarized ^3He Ion Sources and Gas Targets and Their Application (HELION97), Kobe, Japan, 1997 edited by M. Tanaka [Nucl. Instrum Methods Phys. Res. A, **402** (1998)].
- [2] F.D. Colegrove, L.D. Schearer, and G.K. Walters, Phys. Rev. **132**, 2561 (1963).
- [3] M.A. Bouchiat, T.R. Carver, and C.M. Varnum, Phys. Rev. Lett. **5**, 373 (1960).
- [4] L.D. Schearer, F.D. Colegrove, and G.K. Walters, Phys. Rev. Lett. **10**, 108 (1963).
- [5] S.D. Baker, E.B. Carter, D.O. Findley, L.L. Hatfield, G.C. Phillips, N.D. Stockwell, and G.K. Walters, Phys. Rev. Lett. **20**, 738 (1968).
- [6] *Proceedings of the Workshop on Polarized ^3He Beams and Targets*, Princeton, 1984, edited by R. W. Dunford and F. P. Calaprice, AIP Conf. Proc. No. 131 (AIP, New York, 1985).
- [7] O. Karban, S.W. Oh, and W.B. Powell, Phys. Rev. Lett. **31**, 109 (1973).
- [8] R.J. Slobodrian, C. Rioux, and R. Pigeon, Phys. Rev. Lett. **42**, 1401 (1979).
- [9] L.W. Anderson, Nucl. Instrum. Methods **167**, 363 (1979).
- [10] Y. Mori, A. Takagi, K. Ikegami, S. Fukumoto, and A. Ueno, J. Phys. Soc. Jpn. **55**, 453 (1986).
- [11] M. Tanaka, N. Shimakura, T. Ohshima, K. Katori, M. Fujiwara, H. Ogata, and M. Kondo, Phys. Rev. A **50**, 1184 (1994).
- [12] M. Tanaka, M. Fujiwara, S. Nakayama, and L.W. Anderson, Phys. Rev. A **52**, 392 (1995).
- [13] A. Kastler, J. Phys. Radium **11**, 255 (1950).
- [14] J. Brossel, A. Kastler, and J. Winter, Physica (Utrecht) **13**, 668 (1952).
- [15] K. Yonehara, T. Yamagata, T. Takeuchi, Y. Arimoto, and M. Tanaka (unpublished).
- [16] P.G. Sona, Energ. Nucl. (Italy) **14**, 295 (1967).
- [17] H.G. Berry and M. Hass, Annu. Rev. Nucl. Part. Sci. **32**, 1 (1982).
- [18] T. Ohshima, K. Abe, K. Katori, M. Fujiwara, T. Itahashi, H. Ogata, M. Kondo, and M. Tanaka, Phys. Lett. B **274**, 163 (1992).
- [19] A.S. Schlachter, D.H. Loyd, P.J. Bjorkholm, L.W. Anderson, and W. Haeberli, Phys. Rev. **174**, 201 (1968).
- [20] D.R. Swenson, D. Tupa, L.W. Anderson, J. Phys. B **18**, 4433 (1985).
- [21] R.J. Girnius, and L.W. Anderson, Nucl. Instrum. Methods **137**, 373 (1976).
- [22] Y. Arimoto, N. Shimakura, K. Yonehara, T. Yamagata, and M. Tanaka (unpublished).
- [23] T.J. Morgan, R.E. Olson, A.S. Schlachter, and J.W. Gallagher, J. Phys. Chem. Ref. Data **14**, 971 (1985).
- [24] T. Yamagata, M. Tanaka, K. Yonehara, Y. Arimoto, T. Takeuchi, M. Fujiwara, Yu. A. Plis, L.W. Anderson, and R. Morgenstern, Nucl. Instrum. Methods Phys. Res. A **402**, 199 (1998).